NUCLEAR INSTRUMENTS AND METHODS 8 (1960) 27–39; NORTH-HOLLAND PUBLISHING CO.

THE UTRECHT 850 kV CASCADE GENERATOR

I. BEAM DEFLECTION AND ENERGY CONTROL

C. M. BRAAMS and P. B. SMITH

Fysisch Laboratorium der Rijksuniversiteit te Utrecht, Nederland

Received 9 March 1960

The beam deflection magnet and energy control system of the Utrecht cascade generator are described. The uniform-field magnet has entrance and exit slits located outside the magnetic field. Since the cascade generator produces a vertical beam, the most convenient choice for the angle of deflection was 90 degrees. The radius of curvature of the beam in the region of the uniform field is 20 cm, which makes it possible to deflect a one MeV beam of He^+ or D_2^+ ions with a field of 14.5 kilogauss. The whole assembly of the magnet and slits can be rotated about the incoming beam in order to direct the beam to different experimental arrangements. Energy control is achieved in two steps; first the exciting current of the magnet is stabilized, the magnetic field being measured with a proton magnetic resonance fluxmeter, and second the high tension is controlled so as to maintain the deflected beam centered on the exit slit of the magnet. The expected energy resolution of the system has been verified down to an energy spread (full width at half maximum) of 0.15% in proton energy. At this resolution a useful beam (≈ 2 μA) is obtainable with a high-frequency ion source delivering a total beam of about 40 μA protons.

1. Introduction

The Utrecht 850 kV cascade generator has been described previously in several communications[1,2,3]. The latest of these dates from 1955. Since then numerous changes have been made in the associated equipment of the generator, and the generator itself has been converted from 50 Hz to 500 Hz operation. As a result it is now quite suitable for precision work. Since several of the improvements have not been adequately described in published form and since it is felt that such a publication may serve a useful purpose, this, and a companion publication have been prepared. In this article improvements in the beam deflecting and energy control systems will be described. In the second article[4]) will be found details on the beam current integration and measurement.

[1]) W. Maas, Thesis, Utrecht (1948).

[2]) Veenstra, Jongerius, Paris and Valckx, Physica 18 (1952) 378.

[3]) C. H. Paris, Thesis, Utrecht (1955).

[4]) P. J. M. Smulders and P. B. Smith, Nucl. Instr. & Meth. 8 (1960) 40.

[5]) K. T. Bainbridge, Part V, Experimental nuclear physics, editor E. Segrè (John Wiley and Sons, Inc., New York, 1953).

2. The Deflection Magnet

In the following the characteristics of the magnet and its design considerations will be discussed.

2.1. FOCUSSING OF TRAJECTORIES IN THE CENTRAL PLANE

The first-order focal properties of uniform-field sector magnets have been reviewed by Bainbridge[5]). The conditions for stigmatic focussing were first obtained by Cross[6]), and have been worked out in more detail by one of us[7]). We will here summarize some points which are relevant to the construction of the present beam analyzer. Our notation is illustrated in fig. 1. The plane which lies halfway between the parallel pole faces is called the central plane. One of the rays passing through the centers of the entrance- and the exit slit is called the central ray, and we assume that all other rays make small angles with this central ray. Since the divergence of the incoming beam is small and its direction well determined, the

[6]) W. Cross, Rev. Sci. Instr. 22 (1951) 717.

[7]) C. M. Braams, Thesis, Utrecht (1956).

aperture, 2α, of the analyzer is made so small that we can neglect aberrations of second- and higher order in α and will treat only first-order focussing conditions. We also neglect effects of higher order in the quantities s'/r and s''/r, where s' and s'' are the entrance- and exit-slit openings.

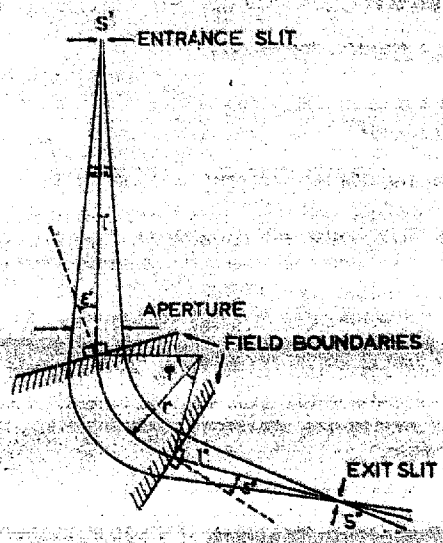

Fig. 1. Schematic representation of deflection magnet, illustrating notation used.

We further use the approximation that the field is uniform within sharp boundaries and zero outside. The entrance- and exit-slits are located at distances l' and l'' from the field boundaries; the normals to the field boundaries at the points of entrance and exit make angles ε' and ε'' with the central ray; in fig. 1 are indicated the directions in which ε' and ε'' are defined as positive. We call $\tan\varepsilon' = a'$ and $\tan\varepsilon'' = a''$. The radius of curvature of the central ray is r and the angle of deflection, φ.

If $\varepsilon' = \varepsilon'' = 0$, i.e., if the field boundaries are perpendicular to the central trajectory at the points of entrance and exit, the condition for the focussing of monoenergetic particles from the entrance slit on the exit slit is expressed by Barber's rule:

$$\tan\varphi = \frac{m' + m''}{r^2 - m'm''}, \tag{1}$$

or, with $\varphi = \frac{1}{2}\pi$:

$$m'm'' = r^2, \tag{1a}$$

where, for normal field boundaries, $m' = l'$ and $m'' = l''$. If ε' and $\varepsilon'' \neq 0$, i.e. for oblique field boundaries, eqs. (1) and (1a) are satisfied by virtual source and image distances, m' and m'', related to the true source and image distances, l' and l'', by the thin-lens formulae

$$\frac{1}{l'} - \frac{1}{m'} = -\frac{a'}{r} \text{ and } \frac{1}{l''} - \frac{1}{m''} = -\frac{a''}{r}. \tag{2}$$

From (1) and (2) the condition for focussing follows:

$$\tan\varphi = \frac{l'(a''l'' + r) + l''(a'l' + r)}{(a'l' + r)(a''l'' + r) - l'l''} \tag{3}$$

which, for $\varphi = \frac{1}{2}\pi$, reduces to

$$\left(a' + \frac{r}{l'}\right)\left(a'' + \frac{r}{l''}\right) = 1. \tag{3a}$$

In what follows we will assume that eq. (3a) is satisfied, i.e., that the slits are located in such a way that monoenergetic particles from a point of the entrance slit are focussed in a point of the exit slit.

If we define the dispersion, D'', as the distance between the central ray with radius of curvature $r + \Delta r$ and the focus for rays with radius r, divided by Δr, this quantity is given by

$$D'' = (l''/r)(\sin\varphi + a'' - a''\cos\varphi) + 1 - \cos\varphi \tag{4}$$

or, if $\varphi = \frac{1}{2}\pi$,

$$D'' = (l''/r)(1 + a'') + 1. \tag{4a}$$

Similarly, we can define a quantity D', which we call the resolution factor, by changing double primes into primes in eqs. (4) and (4a). The total relative momentum spread of particles passing through entrance and exit slits of widths s' and s'' is then given by

$$\frac{\Delta r}{r} = \frac{s'}{D'r} + \frac{s''}{D''r}. \tag{5}$$

A beam analyzer often serves both to collimate the beam and to select the particle momentum. This implies that the entrance slit is fully illuminated by the incoming beam, and that the momentum spread in the unanalyzed beam is greater than that selected by the analyzer. Under these conditions, the intensity of the analyzed beam is proportional to $s's''/D''$,

which for a given analyzer and a given maximum energy spread, i.e., if only s' and s'' are variable, is at a maximum if $s'/D' = s''/D'' = \frac{1}{2}\Delta r$. At this maximum, $s's''/D'' = \frac{1}{4}D'r^2\,(\Delta r/r)^2$, which shows that under the conditions stated above, it is advantageous to choose a design in which D' and r are as large as possible. The design of an analyzer will generally be governed by many, perhaps conflicting, considerations, and no general rules can be given which are valid under all conditions and for all experimental requirements. We feel, however, that in most applications the value of the resolution factor, D', rather than that of the dispersion, D'', is decisive for the performance of our analyzer. The quantities D' and D'' are related to the image magnification, M, by the equation: $M = D''/D'$.

By changing double primes into primes in eq. (4a), one sees that D' increases with l'/r and with a'.

2.2. TWO-DIRECTIONAL FOCUSSING

In section 2.1, we have required without further justification that monoenergetic particles whose trajectories lie in the central plane must produce an image of the entrance slit on the exit slit. The reason is, of course, that this is the condition under which the momenta of the selected rays are independent of their directions. Since the analyzer has no dispersion in the perpendicular, or Z-direction, this does not imply that it should also bring particles whose trajectories make different angles with the central plane to a focus. We have considered three possible requirements with respect to focussing in the Z-direction: a parallel incoming beam may be required to produce either a parallel outgoing beam or a focus at the exit slit, or a source at the entrance slit may be required to be focussed on the exit slit. The first two alternatives may be chosen if the incoming beam is nearly parallel; the last one must be considered if the beam from the accelerator can be focussed on the entrance slit. The present analyzer was designed to produce a stigmatic image of the entrance slit on the exit slit.

Deflection in the Z-direction occurs in the fringing field unless the beam enters and leaves the magnetic field along lines prependicular to the field boundaries. The effect can again be described by thin-lens formulae, stating that Z-deflection occurs in lenses with focal lengths r/a' and r/a'', placed at the points of entrance and exit, respectively. We note that these lenses have the same absolute strengths, but opposite signs as those which, according to eq. (2), describe the effect of oblique field boundaries on the focussing in the central plane. Hence, oblique boundaries act very much like quadrupole lenses. An advantage of the latter is that one has more freedom in choosing their location and strength; a disadvantage, however, that special care is required to assure that their field strength varies proportionally with that in the main magnet, independent of hysteresis and saturation.

Applying the above-mentioned thin-lens formulae, one finds the following relation between the source distance l' and the distance l'' at

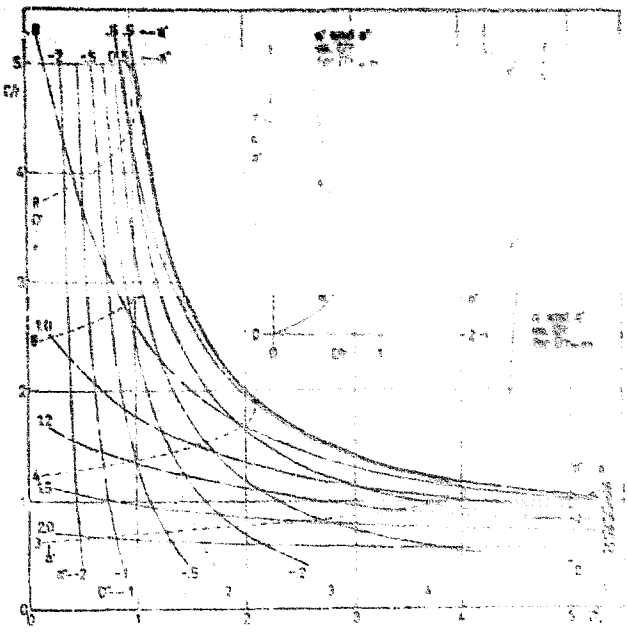

Fig. 2. The focussing condition [illegible] curves of object distance [illegible] against [illegible] (l'',r) for various values of the angles between the normal [illegible] to the field boundaries and the [illegible] radius of curvature of the central ray is given by [illegible]. For the entering beam this angle is given by [illegible] and for the beam at the exit the single [illegible] double primes

which particles with different velocity components in the Z-direction come to a focus:

$$\frac{1}{a' - r/l'} + \frac{1}{a'' - r/L''} = \tag{6}$$

or, for 90-degree deflection:

$$\frac{1}{a' - r/l'} + \frac{1}{a'' - r/L''} = \tfrac{1}{2}\pi . \tag{6a}$$

The condition for stigmatic focussing with a 90-degree deflector is obtained by putting $L'' = l''$ in eq. (6a) and combining it with eq. (3a).

In fig. 2 are shown graphs of l'/r vs l''/r with a' and a'' as parameters. The asymptotic values are plotted in the inserts marked $l'/r = \infty$ and $l''/r = \infty$. This figure is not complete in that curves for $a' < 0.5$ and $a'' > 0.5$ are omitted, while the curves $a' = 0.5$ and $a'' = 0.5$ are only drawn to the left of the point $l'/r = l''/r = 2$, where they touch the envelope. The figure is completed by reflecting it in the line $l' = l''$ and interchanging primes and double primes. We then obtain two sets of values of a' and a'' for every allowed combination of l' and l''.

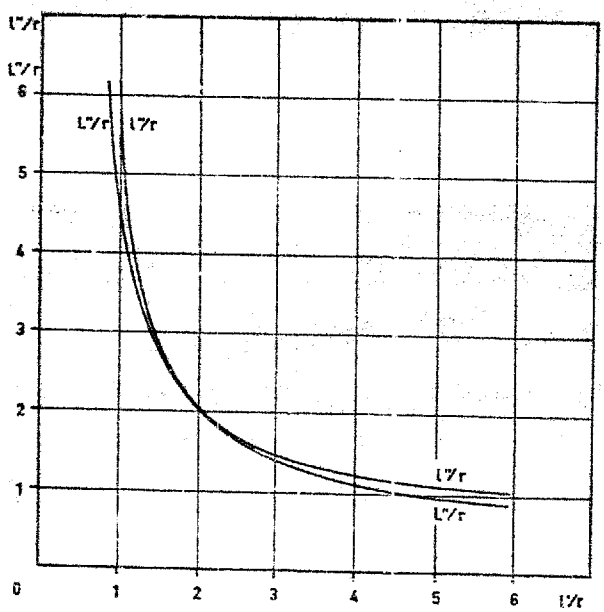

Fig. 3. The image distance in the central plane (l''/r) and in the Z-direction (L''/r) as a function of object distance (l'/r) for the choice of $a' = a'' = 0.5$ used in the design of our magnet. As can be seen the focussing is stigmatic over a relatively large range of values of the object distance.

Dashed and dotted lines in fig. 2 indicate values of D' and D'', respectively.

It is interesting to note that the curves for $a' = 0.5$ and $a'' = 0.5$ run very close together. This suggests that it is possible to obtain approximately stigmatic focussing over a wide range of values of l' and l'' by choosing $a' = a'' = 0.5$. This is borne out by a comparison between the astigmatic image distances l'' and L'' as functions of l', shown in fig. 3. Since moderate deviations from correct Z-focussing do not affect the performance of the analyzer, we have chosen oblique field boundaries with $a' = a'' = 0.5$ for our instrument. This leaves appreciable freedom in the choice of l' and l'' without necessitating the use of adjustable elements, such as a quadrupole lens or semicircular blocks, inserted in the pole faces at the points of entrance and exit.

2.3. DESIGN OF MAGNET AND SLIT SYSTEM

Because of space limitations and also for economy, the analyzer was made as compact as was compatible with the requirement that it should be able to bend a one-MeV beam of singly charged ions of mass number four, which has a momentum of 290 kilogauss-cm. The radius of curvature was, therefore, chosen to be 20 cm. The energy-defining slits were placed at $l' = l'' = 40$ cm; this is a compromise between the requirements that the exit slit and the target, on one hand, be placed as far as possible from the magnet to make room for measuring equipment around the target, and that the entrance slit, on the other hand, be placed at the largest possible value of l', in order to obtain the best possible energy resolution.

The shape of the magnet is shown in fig. 4. The yoke was machined from forged Armco iron and annealed in an inert atmosphere before the final grinding of precision surfaces. The two coils each consist of 1000 turns of 1.5 mm round copper wire, wound on 3 mm thick copper bobbins with 3 mm i.d. copper tubing soldered to the side plates for water cooling. Copper foil of 0.1 mm thickness was wound between successive layers of winding to improve heat conduction from the interior of the coil to the side

plates. The field in the 16 mm wide air gap is 1500 gauss per ampère up to about 10 A; the

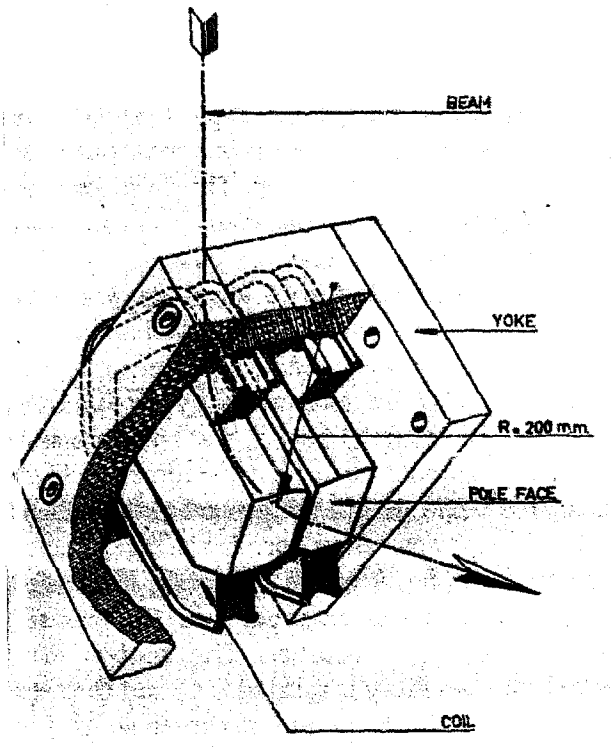

Fig. 4. Cutaway drawing of the magnet construction. See section 2.3 of the text.

coils have run continuously with a current of 12 A, which corresponds to a current density of 3.0 A/mm² averaged throughout the whole cross section of the coil, or 6.8 A/mm² in the windings.

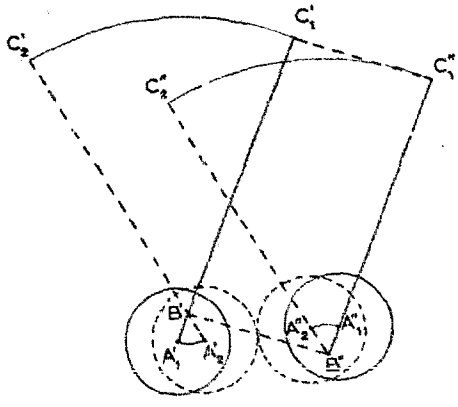

Fig. 5
Operation of the slit system. See section 2.3 of the text.

The design of the pole faces was based on the estimate that the deflection in the fringing field

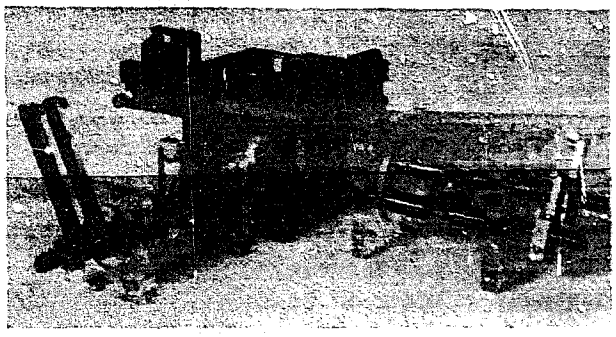

Fig. 6. Photograph of dismounted slit box.

can be accounted for by assuming the uniform field to drop sharply to zero at a boundary lying one gap width outside the pole-face edges. No detailed investigation of the validity of this procedure was made, but provisions have been made for adjusting the position of the slit system with respect to the magnet in case that the focussing should prove to be incorrect.

The slits consist of pairs of cylindrical jaws, which extend into hollow, liquid-cooled shafts, parallel to the cylindrical surfaces. Rotation of the shafts results in a displacement of the excentric jaws and, hence, opens or closes the slits. The operation is shown schematically in fig. 5, which represents a cross section through the slit jaws. The axes of the jaws pass through A′ and A″, the axes of rotation, through B′ and B″. The lever arms B′C′ and B″C″ are of equal lengths and the points C′ and C″ are constrained to move together, the distance C′C″ remaining equal to B′B″. The horizontal projection of the

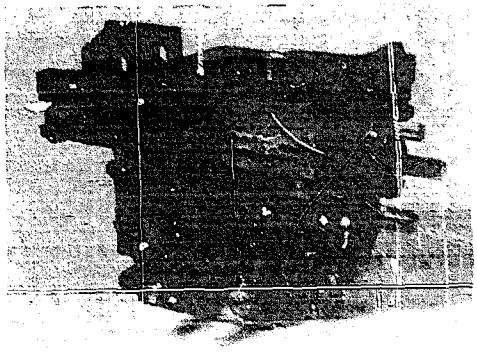

Fig. 7. Photograph of mounted slit box.

displacement of C′ and C″ is proportional to the corresponding variation in the slit opening, as

seen by a vertical beam. This construction also makes the slits open and close symmetrically. The jaws are mounted in lucite plates so that the beam current to each one can be measured or used to stabilize the accelerator voltage. Vacuum seals are made by rubber "o"-rings. An assembly of two perpendicular slits is shown in figs. 6 and 7; the energy-defining slit has a maximum opening of 5 mm and is adjustable with an accuracy of 0.1 mm, while the slit which opens in the Z-direction has a maximum opening of 10 mm, and is adjustable with an accuracy of 0.5 mm. It follows from eq. (5), that the relative energy spread (full width at half maximum), $\Delta E/E = 2\Delta r/r = (s' + s'')/800$, where s' and s'' are the entrance and exit slit openings, measured in mm. The slit jaws were originally made of stainless steel. This proved to be a mistake since the accelerator beam melted them very quickly. After the stainless steel was replaced by silver no further trouble has been found from this source even when sharply focussed 800 keV beams approaching one mA are used.

2.4. ADJUSTMENTS

The following adjustments of the positions of the slit systems with respect to the magnet are possible (fig. 8):

1. each one of the two blocks holding a slit assembly can be rotated slightly about the direction of the beam, so that the energy-defining slits can be placed perpendicular to the central plane;

2. each one can be moved in the Z-direction, so that the center of the slit system can be adjusted to lie in the central plane;

3. the whole frame holding the two slit systems can be moved in the direction of the line in the central plane bisecting the angle between the field boundaries, so that the ratios l'/r and l''/r can be varied simultaneously in the same sense to make them satisfy the focussing condition of eq. (3a);

4. the frame can be rotated about an axis, perpendicular to the central plane and going through the intersection of the lines perpendicular to the field boundaries at the points of entrance and exit, so that the angle of deflection can be adjusted, without the calibration or the focussing being affected.

The first two possibilities for adjustment need little comment except, perhaps, that they are only necessary for one block but were put in for both to preserve symmetry. The third one was necessary because the uncertainty in the fall-off of the field strength near the pole-edge made it impossible to predict with accuracy where the slits should be located for focussing. This adjustment alters the radius of curvature which, however, has to be determined by a calibration anyhow. The fourth, finally, was put in mainly to make it possible to adjust the direction of the analyzed beam within the central plane without change of calibration or focussing. This is illustrated in fig. 9 where P_1 and Q_1 are one set of positions of the entrance and the exit slit, and P_2 and Q_2, another. The center about which the assembly is rotated is C, and the angle of rotation is β. The point C is chosen so, that by this rotation the ray r_1 transforms into the congruent ray r_2. Hence, if we consider r_1 and r_2 as the central rays for the two situations, the rotation leaves l', r, and l'' unchaged. The angles of entrance and exit, however, change by opposite amounts, but it is seen from eq. (3a) that this does not affect the focussing. The ray r_3, which enters through P_2 in a direction parallel to r_1, therefore leaves through Q_2, and it is seen from fig. 9 that it does this under an angle 2β with r_1, except for terms of higher order in β.

The whole assembly of the magnet with its slit system can be moved in the following ways:

5. the analyzer can rotate about a vertical axis, which makes the analyzed beam swing in the horizontal plane;

6. the position of the analyzer on the turntable can be adjusted in two perpendicular horizontal directions to make the entrance slit lie on the axis of rotation;

7. the position of the turntable can be adjusted in two perpendicular horizontal directions to make the beam from the accelerator pass through the entrance slit;

Fig. 8. Representation of the various adjustments possible of the slits with respect to the magnet. See section 2.4 of the text.

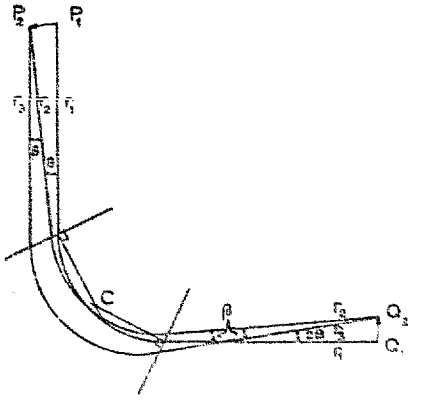

8. the turntable rests on four screws, by which the axis of rotation can be set vertical.

A very simple and compact design of the turntable with its horizontal adjustments was obtained by making use of a commercial ball race with ground flat end-surfaces on which the sliding motions (6 and 7) occur.

Fig. 9. Representation of the turning of rays in the vertical plane as a result of the fourth motion possibility discussed in section 2.4 of the text.

3. The Control System

The present control system, while not original in principle does not seem to have been applied previously to machines of this type, despite the obvious advantage that it presents of delivering to the target monoenergetic ions whose energy is determined by one control knob. The occasion for the development of this system was the conversion of the Utrecht cascade generator from 50 Hz to 500 Hz in the summer of 1957. Previously the ripple on the high tension had been so large (up to 1% at the highest tension) that no practical advantage would have accrued from stabilization.

3.1. PRINCIPLES OF THE CONTROL SYSTEM

A block diagram of the control system is shown in fig. 10. The fundamental comparison voltage is derived from two mercury cells. This is compared to the voltage developed across a standard resistance by the magnet current. The error signal is impressed upon the inputs of two amplifiers in parallel, one an ordinary dc balanced amplifier, and the other a commercial "chopper" type amplifier driving a two-phase motor. The outputs of these two amplifiers are additively mixed, providing, in principle, an ideal integral-plus-proportional controller with no zero setting and essentially infinite zero-frequency gain. This combined output is used to control the field of the dc generator which supplies the main magnet current.

The magnetic field is, of course, not a unique function of the current in the exciting coils. The field varies extemely slowly, however, if the current is maintained constant. The field is measured by a continuous reading nuclear magnetic resonance fluxmeter. Usually the frequency of the fluxmeter is set to the desired value and the magnet current varied so as to centre the absorption dip on a sweep variable in amplitude from zero to about 10 gauss. The field variations encountered are those to be expected in such a system; the long-term stability is within one part in 20 000 for many hours but the inadequate band-pass of the generator permits the occurence of high frequency fluctuations of about one part in 5 000 (average value) most of which are caused by the generator itself.

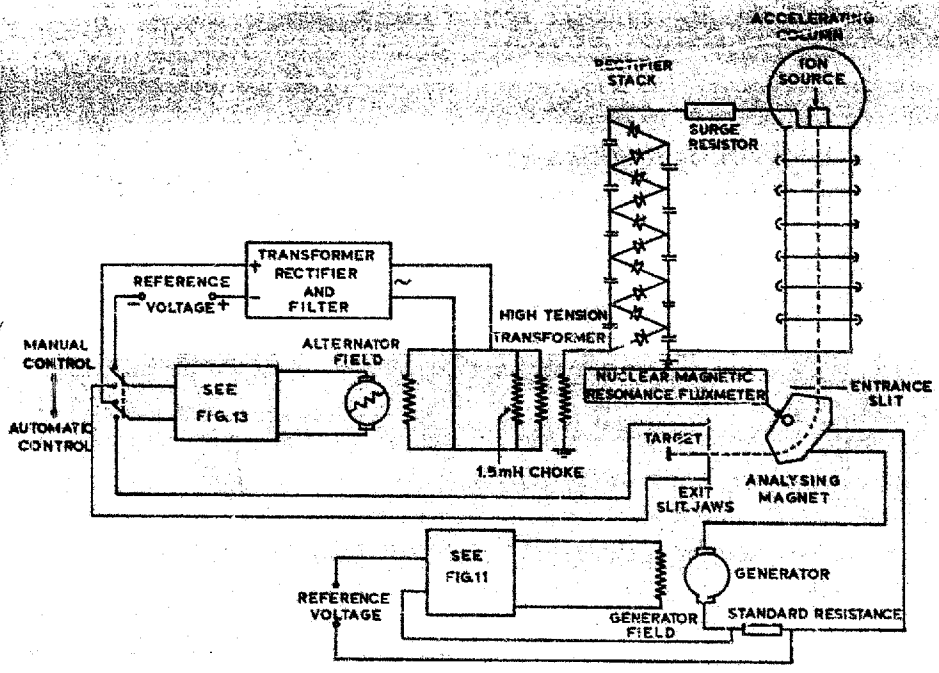

Fig. 10. Block diagram of the complete control and stabilization system of the cascade generator.

A 200 V, 500 Hz, alternator powers the primary of the high-tension transformer of the

cascade generator. The multiplier components, corge resistor, and accelerating tube were not modified during the frequency conversion. The transformer had to be replaced, of course. The new transformer was designed and constructed by N.V. Philips Gloeilampenfabrieken, constructors of the original machine. The large negative reactance reflected into the primary by the multiplying circuit load is partially cancelled by a 1.5 mH air-cored inductance designed and constructed by the Electronics Dept. of the Utrecht Physics Laboratory.

The high tension is controlled by the differential signal developed between the insulated magnet exit slit jaws by the impinging beam. This signal is heavily compensated and then used to control the field of the above mentioned alternator. With this arrangement the beam is controlled by the magnet current, making for extreme simplicity of operation. Alternative manual control of high tension is provided to permit "finding" the beam. Once the beam is through the slits, the high tension may be varied over its entire range by merely changing the magnet current. The system gain is high enough so that no zero setting is necessary, the beam always being at least as great as is obtainable by manual control, and usually greater.

3.2. THE MAGNET CURRENT STABILIZER

The stabilization principle used here is that of paralleling an integrator and an amplifier. In this section it will be shown that analysis of such systems is quite easy, and that a criterion may be found which permits rapid determination of the required gain of the dc amplifier before additive mixing.

The circuit diagram is shown in fig. 11. The analysis is carried out in the complex-frequency (s-) plane. In fig. 11 the transfer functions appropriate to each section of the system are indicated. The additive mixing is accomplished in such a way that, at least to first order, the transmission of each block is unaffected by signal in the other block. Thus the transfer function of the combined amplifiers from the error signal input to the grids marked A and B is given quite accurately by $(A_1 + p_B p_0/s(s+p_0))$. The open-loop pole-zero configuration is shown for the system with $A_1 = 0$, in fig. 12(a). For reasonable values of overall gain the system is unstable, as can be seen by the early crossing of the imaginary axis by the loci of the principal roots of the closed system response.

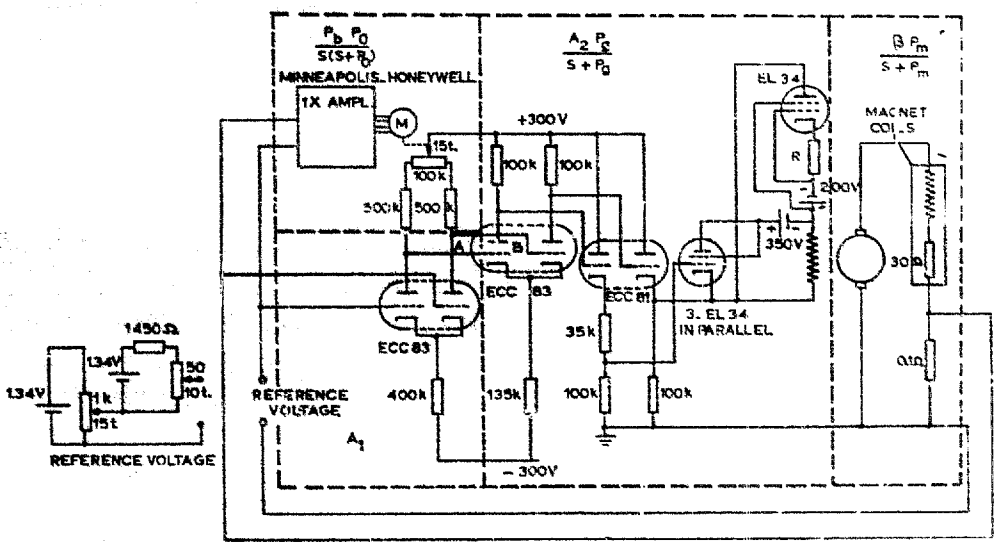

Fig. 11. Circuit diagram of the stabilization circuit of the deflection magnet.

In fig. 12(b) the pole-zero configuration and root loci are shown of the system with $A_1 \neq 0$. It can be seen that for high gain the system is stable due to the two complex zeros arising

from the parallel combination of the two types of amplifiers. Under these conditions the closed loop poles are given approximately by the triangles in fig. 12(b). It can be seen that the

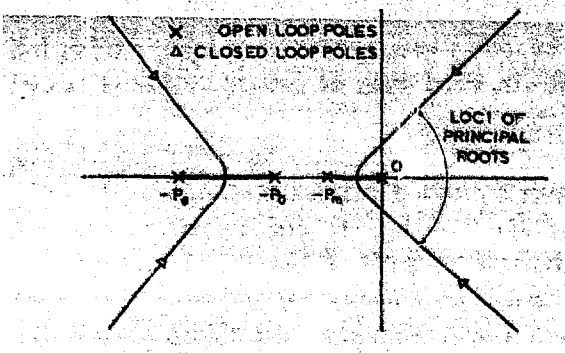

Fig. 12(a). Root loci of the stabilization circuit of the deflection magnet for the case of zero gain of the fast (direct-coupled) amplifier.

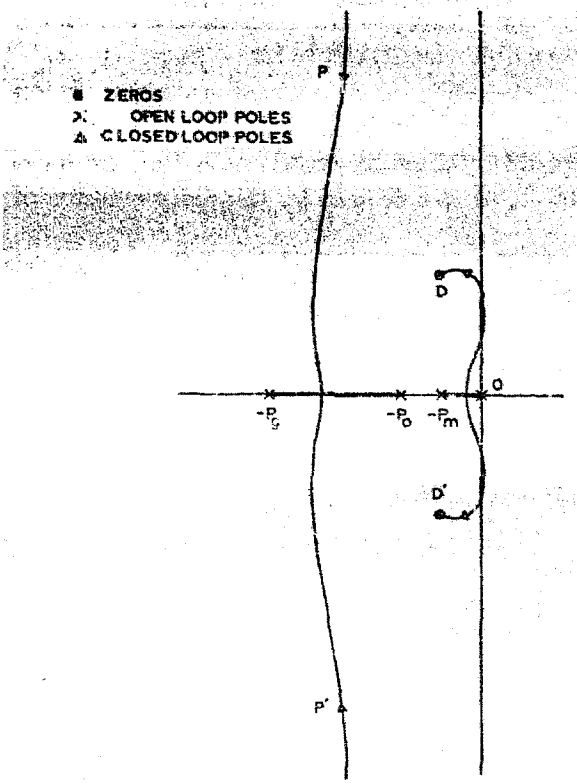

Fig. 12(b). The root loci of the system for $A_1 \neq 0$.

response is governed principally by the high frequency complex conjugate poles P and P'. The dipoles D and D' are quite weak for very high gain, and, although of low frequency, contribute very little to the response of the system (they are, of course, responsible for the high precision). Caution must be exercised i the choice of values of A_1, p_m, and p_B, howeve This can be seen by considering the position o the complex zeros as a function of these variable They are found at $\frac{1}{2}p_0\,(-1 \pm j\sqrt{\gamma -}$ where $\gamma = 4p_B/A_1p_0$. It can be seen from th sketch in fig. 12(b) that for any values of th parameters the system is stable for very hig gain. However, if the imaginary part of th coordinates of zeros is too large, the root lo will go very far into the right half-plane befo returning to the zeros. This results in a cond tionally stable system which may break int sustained oscillation if a temporary overlo drives the system into a region where one o more elements become saturated, thus lowerin the gain so that the right-hand poles move int the right half of the plane. It is probable that similar system described by Havill and Rubin[8] displays this type of behaviour. In their case $A_1 = 1$ which will result in complex zero located very far from the real axis for usua values of p_B and p_0.

In view of the above consideration, meas urements of p_B and p_0 were made on the inte grator used, before the circuit was designed The quantity $\gamma = 4p_B/A_1p_0$ was made equal t approximately ten, resulting in the configuratio sketched in fig. 12(b). For high gain the respons is apparently quite independent of the value o γ, but a more realistic analysis shows this no to be strictly true. The reason that γ cannot b made very small is that the integrator correct for drifts and low frequency flutter noise at th grid of the first amplifier tube. If A_1 is made to large this drift overcomes the correcting capa city of the integrator, and furthermore, th amplifier can drift out of its correct operatin range or the limit of the range of correctio afforded by the integrator.

Thus a correct compromise must be found fo a given case. Fortunately γ can be arbitrarily varied over an enormous range by changing th amplification of the amplifier (A_1) or the gea reduction factor of the integrator (p_B). Th

[8]) J. R. Havill and S. Rubin, Rev. Sci. Instr. 26 1955 515 (N).

behaviour of a correctly designed system is seen to depend principally on the location of the poles P and P′, and to a much lesser extent on the weak dipoles D and D′. In other words this system retains fully the advantages of speed and stability of a simple dc feedback amplifier, while possessing the precision of a chopper type integrating feedback system.

The weak point in the system is the generator. The ripple and noise introduced by this source could be corrected by static or dynamic filters applied to the output. Several such circuits have been described. In this case, however, it would have been better to use direct feed by vacuum tubes or transistors†, since the power consumption is not excessive (less than 5 kW). The generator was used in the present circuit because it already existed when the design was started. The magnetic field variations observed are a factor of five less than the minimum instrumental width utilizable with the cascade generator, and so cause no inconvenience. For that reason no filters (of the types mentioned above) were tried.

3.3. THE HIGH-TENSION STABILIZER

As can be seen from fig. 10, the high tension stabilizer can be operated in two completely diverse manners. The manual control requires no special discussion since the circuit is stable for practically any value of gain. The high tension itself is seen not to be stabilized by this mode of control. In practice it is therefore used only in putting the generator into operation. The automatic control mode would be unstable with any reasonable value of gain and so a discussion is given of the compensation used.

The circuit of the high-tension stabilizer is shown in fig. 13. Only the automatic control mode is shown. The various transfer functions are indicated. It is to be noted that the transfer function of the high-tension rectifier stack is treated as a pure time delay of ½ of one cycle that is 0.001 sec (τ). This approximation is valid for either increasing or decreasing voltage providing the load is adequate. For small load,

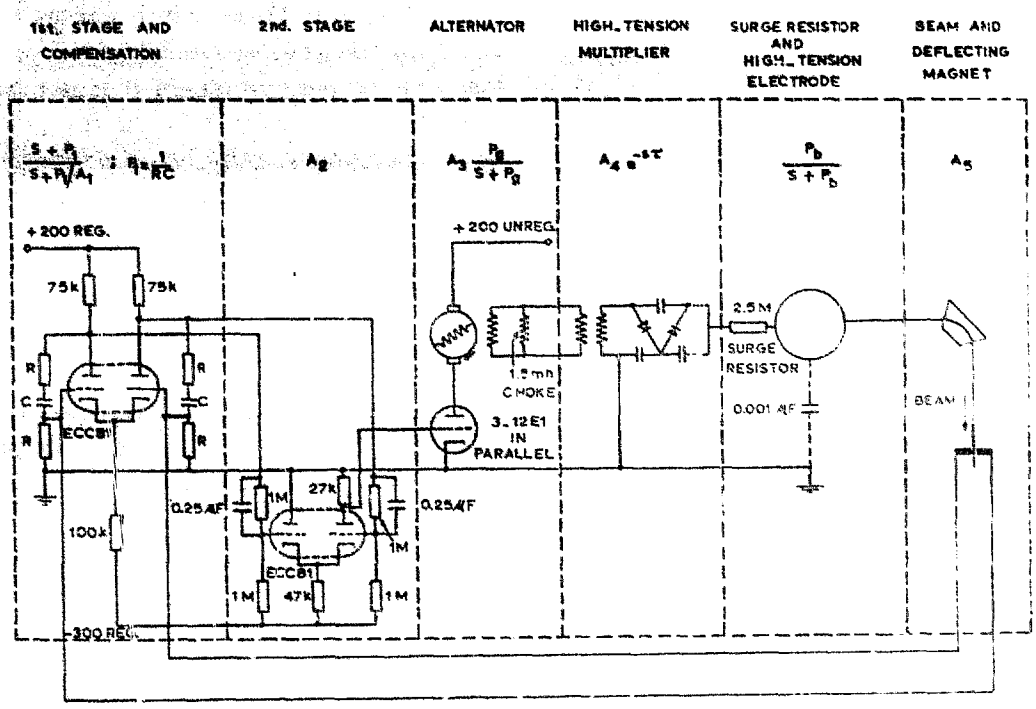

Fig. 13. Circuit of high-tension stabilizer.

† Such a system has since been built at this laboratory for the deflection magnet of the 3 MeV Utrecht Van de Graaff generator. As expected, it shows neither long nor short term fluctuations greater than one part in 25 000.

or large, rapid, changes it ceases to be valid for falling voltage. From the point of view of stability only small changes are usually of importance, however. The generator field time-constant ($1/p_F$) is about 1 sec, and there is also a 2½ millisecond time constant ($1/p_B$) formed by the surge resistor and high-tension electrode capacity.

The various factors shown in fig. 13 are self-explanatory except for A_5, the effective amplification factor of the beam. This is the relation-

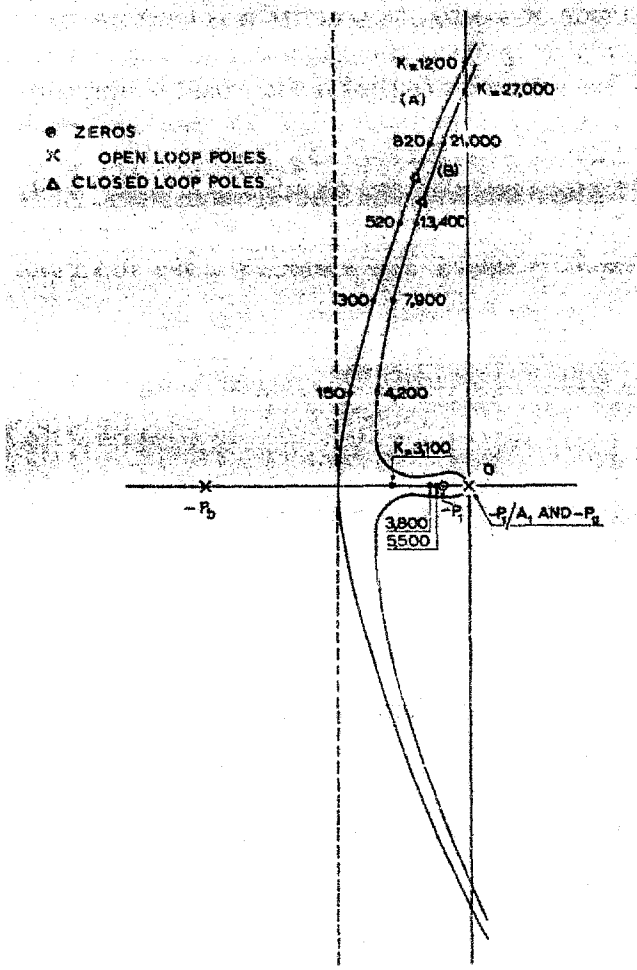

Fig. 14 Root loci for the uncompensated (A) and compensated (B) system.

ship between the change of the high tension and the voltage caused thereby on the slit jaws, through the deflecting action of the magnet. This factor may differ by several orders of magnitude under different circumstances and for this reason the effective resistance to ground of the slit jaws can be changed by the operator to suit conditions.

In order to describe the theory of the circuit a value of A_5 must be specified. In the discussion that follows a typical value will be assumed which renders the zero-frequency loop gain equal to 10^4. This loop gain (K) is given by the product $A_1A_2A_3A_4A_5$. For a value of $K = 10$ the expected deviation of the beam from the center of the exit slit is negligible in comparison with the slit width and the machine ripple.

In fig. 14 the root loci are shown for the uncompensated system (A) (with the condensers C_1 removed) and for the complete system (B). Without the time-lag factor e^{-sT}, the uncompensated root loci would be given by the dashed line. This factor contributes phase-shift which limits the usable gain.

The necessity for the compensation is obvious from an examination of the values of K indicated on the compensated and uncompensated loci. On the scale of fig. 14 it is not possible to show the relative locations of the poles closest to the imaginary axis. These positions and the exact loci in this region are not important, however. For high gain the loci of the principal roots are essentially unmodified by the compensator, the value of K being simply multiplied by A_1 at any given point as a result of the compensation. The values of K indicated on the negative real axis refer to the position of the extra root introduced by the compensation. For $K = 10^4$ this root forms a weak dipole together with the zero at $-p_1$.

Two further details deserve mention. The first is that a provision (not shown) is also made for automatic switching in and out of the control circuit by the beam itself. Circuits to accomplish this are simple to incorporate in the design but should be adapted to conditions likely to be met in the operation of a given machine. Secondly, two phase-lead condensers were incorporated in the coupling networks between the two stages of voltage amplification (fig. 13). These are not strictly necessary (nor very effective) but do produce a desirable effect of speed-up, at least in the manual control mode.

3.4. PERFORMANCE

The magnet, magnet current stabilizer, and high-tension stabilizer have been in operation of

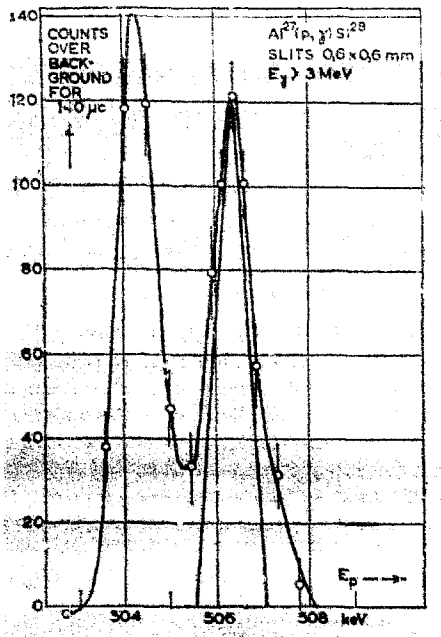

Fig. 15

Gamma-ray yield curve taken with the system described in this article. The reaction under study was $Al^{27}(p,\gamma)Si^{28}$ at the 504–506 keV doublet. See section 3.4 of the text.

a period of more than one year. The most difficult resolution problem encountered in this interval was the study of the 504–506 keV doublet in the Al^{27} (p,γ) reaction. In fig. 15 is shown the yield curve obtained at the time the upper of the two resonances was under study. The triangular resolution curve drawn underneath this resonance is the predicted shape of the yield curve for the slit opening used (0.75 mm) (see section 2.3). The extra width observed is accounted for by the target thickness of several hundred eV (the precise value was not determined). At this slit opening a beam of approximately 2 μA is available on the target located 40 cm beyond the exit slits of the magnet.

Acknowledgements

This investigation is part of the research program of the "Stichting voor Fundamenteel Onderzoek der Materie", and was made possible by financial support from the "Nederlandse Organisatie voor Zuiver Wetenschappelijk Onderzoek".

The authors wish to acknowledge the help and encouragement of their colleagues Prof. Dr. P. M. Endt and Dr. A. M. Hoogenboom. The magnet was constructed in the workshop of the Utrecht Physical Laboratory by Mr. F. A. Meeuwissen, and the stabilizer circuits by Mr. A. Veenenbos.